A new fluorogenic peptide determines proteasome activity in single cells

A New Fluorogenic Peptide Determines Proteasome Activity in Single Cells

Silvana A.M. Urru[1], Pietro Veglianese[1], Ada De Luigi[1], Elena Fumagalli[1], Eugenio Erba[1], Rodolfo Gonella Diaza[1], Andrea Carrà[1], Enrico Davoli[1], Tiziana Borsello[1], Gianluigi Forloni[1], Niccolò Pengo[2],
Enrico Monzani[3], Paolo Cascio[4], Simone Cenci[2], Roberto Sitia[2], Mario Salmona[1*]
[1] Istituto di Ricerche Farmacologiche "Mario Negri", Via La Masa 19, Milan 20156, Italy.
[2] Division of Genetics and Cell Biology, San Raffaele Scientific Institute and Università Vita-Salute San Raffaele, Via Olgettina 60, Milan 20132, Italy.
[3] Department of General Chemistry, University of Pavia, Via Taramelli 12, Pavia 27100, Italy.
[4] Department of Veterinary Morphophysiology, University of Turin, Via Leonardo da Vinci 44, Grugliasco (TO) 10095, Italy.
*To whom correspondence should be addressed E-mail: mario.salmona@marionegri.it, Phone: +39 02 39014447, Fax: +39 02 39014744
Abbreviations: UPS, ubiquitin proteasome system; Ub, ubiquitin; TED, TAT-EDANS-DABCYL; FRET, fluorescence resonance energy transfer; GFP, green fluorescent protein; FACS, fluorescenceactivated
cell sorting; MALDI-TOF-MS, MALDI-time-of-flight mass spectrometry

Abstract
The ubiquitin-proteasome system plays a critical role in many diseases, making it an attractive biomarker and therapeutic target. However, the impact of results obtained *in vitro* using purified proteasome particles or whole cell extracts is limited by the lack of efficient methods to assess proteasome activity in living cells. We have engineered an internally quenched fluorogenic peptide with a proteasome-specific cleavage motif fused to TAT, and linked to the fluorophores DABCYL and EDANS. This peptide penetrates cell membranes and is rapidly cleaved by the proteasomal chymotrypsin-like activity, generating a quantitative fluorescent reporter of *in vivo* proteasome activity, as assessed by time-lapse or flow cytometry fluorescence analysis. This reporter is an innovative tool for monitoring proteasomal proteolytic activities in physiological and pathological conditions.

Introduction
The ubiquitin proteasome system (UPS) has a fundamental role in maintaining cell viability, by regulating the turnover of cell proteins [1-4]. Its proteolytic activity provides an essential quality control mechanism that selectively eliminates misfolded or damaged proteins. In addition, because the proteasome also degrades regulatory proteins, it has an impact on virtually all biological processes, including regulation of gene transcription, cell cycle progression, apoptosis, development and
differentiation. Finally, the proteasome generates immunogenic peptides that are presented on the cell
surface, making it a key factor in self-recognition and adaptive immunity.
Altered proteasomal activity has been implicated in many diseases, ranging from neurodegenerative disorders, to genetic diseases, cardiac dysfunction and autoimmune syndromes [3,5,6]. Specific changes in
UPS have been identified in cancer, where aberrant regulation of cell cycle proteins can lead to

tumorigenesis [3,6,7]. For this reason, the development of proteasome inhibitors as new anti-tumor agents [8-10] represents a promising therapeutic strategy, as demonstrated by the success of bortezomib, a drug approved for the treatment of multiple myeloma [11].

The efficacy of new molecules with therapeutic potential is usually evaluated using *in vitro* systems with purified components of the proteasomal system [12,13]. However, results obtained by these methods may be misleading, because they measure only certain features of proteasomal degradation, and do not account for important parameters, like cell permeability, solubility, and bioavailability, as well as effects from interaction with other cellular components.

To evaluate proteasomal activity in intact cells and *in vivo*, fluorescent proteasome substrates have been engineered [14-16], and have been powerful tools for investigating proteasome insufficiency and studying disease models in which mutant proteins overload the proteasomal capacity. However, these reporters cannot detect physiological fluctuations in the level of proteasome expression and functional workload, which may have profound biological implications. Moreover, accumulation of ubiquitin-GFP reporters depends not only on proteasomal activity, but also on the efficiency of their expression and ubiquitination. Finally, techniques that rely on expression of fusion proteins are not suitable for monitoring proteasome activity at the single cell level, or for routine diagnostics, for example in primary human samples. Therefore, a compelling need exists for *in vivo* methods for quantitating proteasomal activity.

In this study, we used an innovative approach to engineer an internally quenched fluorogenic peptide, TAT-EDANS-DABCYL (TED), that is specifically recognized and hydrolyzed by β5, the main proteosomal subunit responsible for the chymotrypsin-like activity [17,18], the main proteasomal activity and the rate limiting activity in proteins turnover *in vivo*. Due to its short sequence (20 residues) TED diffuses freely into the proteasomal proteolytic core and therefore its degradation *in vivo* is most likely independent of preliminary ubiquitination [19]. Furthermore, TED enabled the direct determination of proteasome efficiency in living cells, using fluorescence microscopy and flow cytometry. In fact the core-structure of the peptide was fused to a TAT sequence that allows the construct to efficiently penetrate biological membranes [20,21], thus circumventing the need for a complex macromolecule delivery strategy, such as viral transduction or microinjection. We added the feature of internal quenching by introducing the donor/acceptor pair DABCYL/EDANS [22], that allowed to easily follow fluorescence changes using the fluorescence resonance energy transfer (FRET) technique.

Here we show that TED is a useful tool for fast and simple evaluation of proteasomal activity in living cells, and provides the possibility for *in vivo* monitoring of altered proteasome activity at the single-cell level in patient-derived cells.

Results

Characteristics of Engineered TED Peptide. The schematic structure of TED is shown in Figure 1.

The strategy for designing the peptide comprised the following steps:

1. Incubation of commercial Suc-LLVY-amc with purified 26S proteasome for 22 h caused complete degradation of the substrate, as demonstrated by HPLC/MS-MS. Figure S1 shows the proportions of the different proteolytic fragments of the peptide, with the most abundant (85%) derived from cleavage at the C-terminal site of the Tyr residue (Table S1). This showed for the first time that proteasomal cleavage of the prototypic substrate for chymotrypsin-like activity occurs primarily at the Tyr-amc bond.

To mimic this effect, Leu-Leu-Val-Tyr (LLVY) was chosen as the "cleavage-determining motif", because it is preferentially cleaved at the Tyr residue by the chymotrypsin-like activity of the proteasome [23,24].

2. To further promote specific cleavage at the Tyr residue, a bulky side chain was added close to the Cterminus of the scissile motif [25,26]. We chose to link the EDANS moiety to the side chain of the Glu residue at position 10.

3. Residues 48-57 of the transfer domain from the TAT protein were fused to the peptide C-terminus to provide cell membrane-penetration capacity [27].

4. Lys and Arg residues promote cell membrane crossing [28], so N-terminal residues were selected to maximize penetration by adding three Lys residues flanking the Leu at position 5. This gave the peptide a net positive charge, as shown by surface charge distribution modeling (Figure S2).

5. To minimize the possibility of N-terminal degradation, the Lys residues at positions 1, 3 and 4 were in the D conformation.

6. For internal quenching, a DABCYL group was bound to Lys at position 2, and EDANS to Glu at position 10. The structural model of TED was analyzed with molecular dynamic simulations (Figure S2), showing a very mobile structure, with no conformations that were more stable or preferred in the solvated environment. The fluorophore pair distance, as measured by PyMOL, was between 7 and 30 Å, which was lower than their Forster radius (R_0 = 33 Å), the distance at which the energy transfer efficiency is 50% [22].

The purity of TED was always above 98% as determined by HPLC analysis (Figure S3) and peptide identity was confirmed by specific analytical methods such as NMR and high resolution mass spectrometry analyses (Figures S4-S6 and Table S2).

To assess if proteasomal cleavage of TED occurred specifically at the Tyr residue of LLVY, as it did in Suc-LLVY-amc, the peptide was added to HeLa cells. After 15 min, cells were collected and lysed, and the main peptide cleavage products purified and identified by reverse phase HPLC and MS. Representative mass spectra from HeLa cell lysates are reported in Figure 2, similar results were obtained for U266 and MM.1S multiple myeloma cell lines. The molecular ion at m/z 3084.48 $[M+H]^+$ that is characteristic of TED (Figure 2A) was almost negligible after cell incubation, indicating efficient degradation (Figure 2B). The most abundant proteolytic fragment, at m/z 1270.97,

corresponded to the peptide obtained by cleavage of TED at the carboxyl end of the Tyr residue at position 8. The mass spectra also clearly showed a proteolytic fragment at m/z 1141.58, corresponding
to cleavage at both the Tyr residue and the N-terminal Lys residue. No evidence of cleavage between
Lys(DABCYL) residue at position 2 and D-Lys residue at position 3 was found (Figure 1). These results indicated that separation of the DABCYL/EDANS pair is observed only when proteolysis occurs at the Tyr residue, confirming that specific proteasomal cleavage caused the appearance of the
fluorescent signal.

Internalization and Cleavage of TED in Living Cells. We next evaluated TED as a reporter of proteasomal activity in primary hippocampal neurons, and in different tumor cell lines, specifically HeLa, a human cervical carcinoma line; N2a, a mouse neuroblastoma; and MM.1S and U266, two human multiple myeloma cell lines. Proteasomal cleavage of TED led to physical separation of the DABCYL/EDANS pair, abolishing intramolecular quenching, with increases in EDANS fluorescence
proportional to the amount of substrate cleaved. Optical microscopy imaging using time-lapse recording and image analysis were performed on adherent cells, or cells in suspension after plating. After 5 min of incubation with 17 μM TED, time-lapse experiments showed a progressive increase in
EDANS-fluorescence in most cells, reaching a maximum value within 15 min (Figure 3A and Figure
S7A). The percentage of fluorescent cells varied between 38% in MM.1S cells and 87% in hippocampal neurons (Table 1). The half-life of the fluorescent signal was determined to be 60 min (data not shown).

Changes in fluorescence signal were evaluated in parallel by FACS on U266 and MM.1S cell lines growing in suspension. TED cleavage in multiple myeloma cell lines was comparable to that observed
by time-lapse recording, the frequency of fluorescent cells was 47.4% in U266 and 35% in MM.1S, indicating the versatility of this reporter. To further ascertain that fluorescence resulted from proteasomal activities, we used an engineered U266 human multiple myeloma cell line stably expressing a destabilized GFP fused to a mutated uncleavable Ub moiety (Ub^{G76V}GFP-U266 cells) [33].

This is an established short-lived substrate, that accumulates upon pharmacological inhibition or functional overload of the proteasome [14,33]. No increased toxicity following exposure to proteasome inhibitors or TED was observed in Ub^{G76V}GFP-U266 cells [33] (data not shown). Following incubation of
cells with TED, FACS analysis showed that EDANS but not Ub^{G76V}GFP fluorescence was evident; conversely, pretreatment with epoxomicin led to a significantly decreased EDANS fluorescence and GFP accumulation (Figure 3C). The inverse correlation between EDANS and GFP fluorescence demonstrated that TED is degraded by the proteasome.

To determine whether the fluorescent signal was specifically due to proteasomal cleavage of TED, prior to peptide administration cells were incubated for 3 h with 5 μM epoxomicin, a specific and irreversible proteasome inhibitor [29]. Epoxomicin treatment resulted in a significant decrease in fluorescence in HeLa, N2a, MM.1S, U266 cells and primary hippocampal neurons (Table 1; Figure 3B and Figure S7B). Its efficacy in inhibiting TED cleavage ranged between 40 and 78%, which correlated
with the sensitivity of the different cell types to the drug [30-32]. In light of these observations we performed dose-response experiments to determine the IC50 values for epoxomicin, and two reversible
and widely used proteasome inhibitors, MG-132 and bortezomib [32]. As shown in Figure 4 all three

molecules inhibited proteasomal activity in HeLa cells; epoxomicin and MG132 had a similar potency,
IC50 were 13.08 μM and 6.45 μM respectively, while bortezomib showed a much greater potency with
an IC50 of 141.3 nM (p=0.0016, F=14.26).

Intracellular Localization of TED. Optical microscopy with time-lapse recording was used to evaluate the intracellular distribution of TED fluorescence. In primary hippocampal neurons, and in N2a and HeLa cell lines, we observed a prevalent nuclear distribution, as indicated by co-localization
of EDANS with SYTO59 nuclear staining (Figure 5 and Figure S8). Both multiple myeloma lines showed similar fluorescence intensity in the cytoplasm and nucleus (Figure 5 and Figure S8). Time-lapse recording allowed the monitoring of progressive changes in the distribution and intensity of
fluorescent signals in different cell compartments. Fluorescence was initially concentrated in the cytoplasm of both hippocampal neurons and MM.1S cells. Signal increased progressively in the primary neuron culture until nuclear localization was prevalent, while a more homogeneous distribution between cytoplasm and nucleus was maintained in MM.1S cells (Figure S9).

TED Detects Differential UPS Efficiency in Different Human Multiple Myeloma Cell Lines. We
next tested the reporter in multiple myeloma cell lines. The MM.1S line is exquisitely bortezomibsensitive,
because it expresses fewer proteasomes, which have a higher functional workload than in U266 cells [33]. We reasoned that the reporter might discriminate between sensitive and resistant multiple
myeloma cell lines by detecting idle proteasomes, so we quantified TED processing in these two lines.

As shown in Figure 6, U266 cells showed a higher fluorescence intensity at each time point after incubation with 17 μM TED, suggesting that MM.1S cells were less efficient at cleaving the reporter.

The impaired degradation of TED that we observed in MM.1S cells is consistent with the reported imbalance between proteasomal workload and degradative capacity in these cells [33].

Discussion

Proteasome activity in living cells can be assessed indirectly by a number of approaches. The development of fluorogenic peptides to evaluate the three main peptidase activities of the 26S particle,
enables proteasomal enzymatic capacity to be determined in cell extracts [13], so allowing proteasomal
complements to be compared in different cell types [33-35]. However, the proteasomal complement may
be adequate under normal physiological conditions, but inadequate in cells expressing aggregationprone
proteotoxins, or in situations that increase the demand for proteasomal degradation [36,37].

UPS efficiency can be inferred by measuring the half-life of proteasomal substrates. Similar information can be obtained by assessing the steady-state levels of Ub-conjugates or free Ub, by immunoblotting or autoradiography, especially in pathological conditions that challenge and overload
proteasome function [38,33]. However, these classical biochemical assays do not allow direct assessment
of UPS efficiency *in vivo*. They are also demanding and time-consuming, and therefore they cannot be
adopted for routine diagnostics of primary samples.

As an alternative, fluorescent probes have been developed to measure UPS insufficiency. By coupling
the degradation signal to GFP, rapid ubiquitination and proteasome-dependent degradation can be observed [15]. These reporters efficiently detect proteasome inhibition and overload *in vitro* and *in vivo*,
proving powerful means of assessing toxicity in disease models [39]. However, destabilized GFPs fail to
ascertain the exact step in the UPS that is impaired under pathological or stress conditions, and have proven inadequate for reporting on physiological fluctuations of UPS efficiency. Finally, their use require transient or stable transfection or transduction of the analyzed cells [40].
More recently, a cell-based assay that employs bioluminescent synthetic peptides in a coupled-enzyme
format has been proposed for evaluating the three ®-peptidase catalytic activities [41]. However, this assay requires weak permeabilization of the cell membrane, which may interfere with cell function.
We attempted to overcome these limitations in UPS assessment by engineering the new peptide TED as
a tool for evaluating proteasomal activity in intact living cells. TED has a TAT sequence that allows it
to directly cross cell membranes. Combined with FRET, TED allows measurement of proteasomal activity in living cells after simple addition of the peptide to cell suspensions or culture media, without
membrane permeabilization. TED abolishes the requirement for altering cell permeability and structure, and allows direct and quantitative evaluation of proteasomal activity by measuring the appearance of fluorescence. Although some fluorescence is generated independently of proteasome activity as an indication that experiments cannot entirely rule out a minor contribution by other proteases to observed fluorescence, our data show significant cleavage attributable to the proteasome.
MS analysis confirmed that cleavage was specifically mediated by the chymotrypsin-like activity, at the Tyr residue of the prototype motif LLVY.
In contrast to GFP-based reporters, TED is a short peptide that does not require ubiquitination for degradation by the proteasome [19]. Real-time monitoring of TED fluorescence, for example by timelapse
microscopy or repeated FACS analysis, allows kinetic evaluation of proteasomal activity in living cells, during basal or challenged conditions.
The potential applications of TED in basic and translational research are manifold. In this study, we compared UPS efficiency in two multiple myeloma cell lines recently shown to possess different levels
of proteasomes and functional workload [33]. Fluorescence was higher in the multiple myeloma cell line
with higher activity and lower workload, suggesting a role for TED as a reporter of proteasome idleness. The imbalance in proteasome load and capacity that was observed in these multiple myeloma
cell lines coincided with apoptotic sensitivity to proteasome inhibitors, so TED might be employed to
predict sensitivity to bortezomib in primary multiple myeloma patient-derived samples, and perhaps in
other cancers. Indeed, although the proteasome inhibitor bortezomib has been successful as a multiple
myeloma therapy, the molecular basis for differences in individual responsiveness remain obscure, and

no predictive factor for successful treatment has been identified. More generally, TED might be useful
for investigating conformational diseases marked by altered proteasomal activity, such as neurodegenerative disorders [5].
Impairment of proteasome activity induces alternative proteocatabolic pathways like autophagy, which
has important implications for neurodegeneration [39,42,43]. The molecular sensors and networks linking
UPS and autophagy are still unclear, thus TED may be valuable for monitoring the onset of proteasome
impairment in disease models, for gaining mechanistic insights into the activation of autophagy.
Another potential biotechnological application of TED is the measurement of rapidly degraded polypeptides (RDP). These constitute a significant proportion of total proteins, and are degraded soon
after synthesis, imposing a significant load on proteasomes [44]. RDP measurement relies on radiometabolic pulse-chase labeling and trichloracetic acid (TCA)-precipitable radioactivity assessment
in the presence of proteasome inhibitors. More direct and reliable assays are needed for studying the role of RDP in cell function and immunity. Importantly, TED might allow direct measurement of RDP
by quantifying rapid changes in fluorescence by microscopy or FACS, after pharmacological blockade
of protein translation.
The ability to monitor TED fluorescence in living cells also allows the observation of changes in the intracellular distribution of proteasomal activity. We found that primary neurons had a mainly nuclear
distribution, and that multiple myeloma cells had equal distribution in the cytoplasm and nucleus. TED
can be applied directly to living cells, excluding the possibility of artifactual uptake, or nuclear localization due to fixation [45].
In conclusion, our study demonstrates that TED is an important technological development for investigating proteasomal activity in living cells. It should advance the analysis of the UPS in physiology and pathology, in both basic research and clinical applications, including diagnostics, new
biomarkers and novel therapies.

Conclusions

The ubiquitin proteasome system (UPS) is vital for maintaining cell viability, regulating the turnover of
cell proteins and providing the quality control mechanism that selectively eliminates misfolded or damaged proteins. Altered proteasomal activity has been implicated in many diseases, such as neurodegenerative disorders, genetic diseases, cardiac dysfunction and autoimmune syndromes. The efficacy of new molecules with therapeutic potential aimed at controlling aberrant regulation of cell cycle proteins is usually evaluated using *in vitro* systems with purified components of the proteasomal
system. However, these methods may give misleading results, because they only measure limited features of the proteasomal degradation mechanism. To evaluate proteasome activity in intact cells and
in vivo, fluorescent substrates have been engineered but they are unable to detect the physiological fluctuations of its expression and functional workload, which may have profound biological implications. Moreover, techniques that rely on expression of fusion proteins are not suitable for monitoring proteasomal activity at the single cell level, or for routine diagnostics, for example in

primary human samples. We report an innovative approach to engineer an internally quenched fluorogenic peptide, that is specifically recognized and hydrolyzed by β5, the proteosomal subunit responsible for the chymotrypsin-like activity, and does not require ubiquitination to be a proteasomal
substrate. This peptide permits direct determination of proteasome efficiency in living cells, using fluorescence microscopy and flow cytometry. Its core structure is fused to a TAT sequence that enables
the construct to efficiently penetrate biological membranes so changes in the intracellular distribution
of proteasomal activity can be seen as well. It can be applied directly to living cells, excluding the risk
of artifactual uptake or nuclear localization due to fixation. This reporter can advance analysis of the
UPS in physiology and pathology, in basic research and clinical applications, including diagnostics, new biomarkers and novel therapies.

Experimental Section

TED Synthesis and chemical characterization. TED (H-DLys-Lys(DABCYL)-DLys-DLys-Leu-Leu-
Val-Tyr-Gly-Glu(EDANS)-Gly-Arg-Lys-Lys-Arg-Arg-Gln-Arg-Arg-Arg-OH) was synthesized using
solid-phase FMOC chemistry on an Applied Biosystems 433A synthesizer, and purified by reverse phase HPLC with a Symmetry C4 column (150 × 19 mm, 300 Å, 7 μm; Waters) on an ÄKTA purifier
10 XT instrument (GE Healthcare). Identity and purity were determined both by tandem mass spectrometry (MS/MS) and by MALDI-time-of-flight (TOF) mass spectrometry (MS). MS/MS analysis have been performed with a high resolution mass spectrometer LTQ Orbitrap XL hybrid FTMS (Fourier Transform Mass Spectrometer) by direct infusion of TED with a Prosolia electrospray
ionization (ESI) ion source. MALDI-TOF experiments were carried out with a Bruker Reflex III timeof-
flight (TOF) mass spectrometer operating in the linear mode. TED purity was also checked by HPLC using an ÄKTA purifier 10 XT instrument (GE Healthcare) equipped with a C4 column (250 x
4.6 mm, 300 Å, 7 μm; Vydac) and UV/vis detector (214 and 460 nm). The retention time was 27 min,
in gradient solvent elution (H_2O + 0.1% TFA / CH_3CN + 0.08% TFA; 95:5% for 6 min, 65:35% in 18
min, 65:35% for 5 min, 60:40% in 8 min, 60:40% for 2 min, 0:100% in 3 min, 95:5% in 3 min, 95:5%
for 10 min) at the flow rate of 0.5 ml/min.TED purity was always higher than 98 %. Peptide was lyophilized and stored at -80 °C. Reagents were obtained from Novabiochem.

^{1}H-NMR and ^{13}C-NMR characterization data of the aromatic residues of TED. ^{1}H, ^{1}H-^{1}H DQFCOSY,
and ^{1}H-^{13}C-HSQC spectra of TED dissolved in D_2O were recorded at 25 °C on a Bruker AVANCE 400 spectrometer, operating at 9.37 T. ^{1}H and ^{13}C resonances, together with the coupling constants of aromatic residues were recorded. The large overlapping of the signals prevented the assignment of the aliphatic resonances.

Determination of Suc-LLVY-amc and TED Cleavage Products. Succinyl-Leu-Leu-Val-Tyraminomethylcoumarin
(Suc-LLVY-amc, Bachem) degradation was performed as previously described

[46]. Briefly, 200 μM Suc-LLVY-amc in 40 mM Tris, pH 7.5, 2 mM ATP, 4 mM $MgCl_2$. was incubated
for 22 h at 37 °C in the presence of 2.5 μg of 26S proteasomes, purified as reported [38]. Reactions were
stopped by cooling, peptides separated by filtration through a 3000 Da Microcon device (Millipore) and analyzed with an Agilent 6410 Triple Quadrupole LC/MS system, with a Chromolith FastGradient
RP-18 endcapped 50-2 column (1.6 μm, 130 Å; Merck Chemicals).
A solution of 17 μM TED, dissolved in water:acetonitrile (1:1), was added to cell culture medium and
incubated for 15 min at 37 °C; medium was removed, cells were washed with phosphate buffered saline (PBS), detached and recovered by centrifugation. The pellet was resuspended in PBS, cells were
lysed by freeze-thawing, centrifuged at 3000 ×g for 5 min and the supernatant used for analysis. Fragments from TED degradation were identified and analyzed by reverse phase HPLC and MALDITOF
MS.
Molecular Modeling. Models were built and analyzed with MacroModel (Schrodinger). The simulated
system consisted of TED in a cubic box at a distance of 3.0 nm from its periodic image, with approximately 30,200 molecules of water. System energy was minimized with the steepest descent algorithm, with subsequent refinement with a conjugate gradient, followed by a 100 ps of equilibration
to generate the starting point for molecular dynamics. The OPLS2001 force field was used, and all simulations were carried out at 298 K temperature and 1 atm pressure [47]. Multiple conformations were
stored at regular intervals for subsequent analysis. Electrostatic potential was calculated using the DelPhi program v.4 [48], with finite difference solution to the nonlinear Poisson-Boltzmann equation, and
visualized using PyMOL software (http://pymol.org).
Cell Lines. Cells were cultured in DMEM (HeLa and N2a) or RPMI 1640 (U266 and MM.1S), both
supplemented with 10% heat-inactivated FCS, 2 mM L-glutamine, 100 U/ml penicillin and 100 μg/ml
streptomycin and maintained in humidified air at 37 °C with 5% CO_2. Reagents for cell culture were
obtained from Invitrogen. U266 cells stably expressing a destabilized GFP fused to a mutated uncleavable ubiquitin moiety (Ub^{G76V}GFP) were cultured as previously described [33]. Primary hippocampal neuron cultures were prepared from 2-day-old rat pups as previously described [49].
Cell Treatments. Hippocampal neurons were plated on polylysine coated 8-wells μ-Slides ($1x10^5$ cells/well) and used after 11-13 days in culture. Confluent cell lines were detached by trypsinization, centrifuged, resuspended in medium without phenol red and plated as above ($1\text{-}5x10^5$ cells/well) and
used after 72 h. TED in water:acetonitrile (1:1) was added to the medium at a final concentration of 17
μM, and cells were used immediately for optical microscopy cell imaging. Pretreatment with proteasome inhibitors was with 5 μM epoxomicin or 25 μM MG-132 (Novabiochem), in DMSO, at 37
°C for 3 h, or for 2 h for MM.1S cells, which have higher sensitivity to proteasome inhibitors [30]. For dose-response studies, proteasome inhibitors in the range of 0.5- 20 μM for epoxomicin, 1 - 20 μM for

MG-132 and 0.01 - 1 μM for bortezomib (MG-341, LC Laboratories) were added to culture medium 3
h before incubation with TED.

Flow Cytometry Analysis. After incubation with TED in the presence or absence of 5 μM epoxomicin, MM.1S and U266 cells were pelleted, resuspended in 1 ml of PBS and analyzed with a fluorescence-activated cell sorting (FACS) Vantage Instrument equipped with a Enterprise UV/488 nm
laser (Becton Dickinson). Fluorescence pulse was detected at 580 ± 30 nm and each flow cytometric
analysis was performed on at least 20,000 cells. Data were analyzed with CellQuest (Becton Dickinson) software.

Optical Microscopy and Time-lapse Recording. Adherent cells were detached by trypsinization, centrifuged, resuspended and plated on polylysine coated μ-Slides as described above, and grown in humidified air at 37 °C with 5% CO_2, to 60% confluence. Cells were treated with 17 μM TED and immediately analyzed. For co-localization experiments, the cell nucleus was stained with SYTO59 (Invitrogen) at a final concentration of 1 μM. Images were collected and analyzed with a Cell^R imaging
station (Olympus) coupled to an inverted microscope (IX 81, Olympus) equipped with an incubator to
maintain constant temperature (37 °C) and CO_2
(5%) values. The EDANS fluorescent signal was
acquired with a high resolution camera (ORCA) equipped with a 340 nm excitation filter (D340xv2 Chroma), a 400 nm dichroic mirror (400DCLP, Chroma) and an emission filter with a range of 510 ±
40 nm (D510/40m, Chroma). Images were acquired after 15 min of incubation and 10 different frames
randomly sampled for a minimum of 100 cells. EDANS-positive cells, identified after removing background, were counted and compared to the total cell number counted by bright-field.

Statistical Analysis. Significant differences between treatment groups were evaluated with an unpaired
t-test with equal variance to calculate a two-tailed *P*-value. For the determination of IC50 values of proteasome inhibitors (i.e. the concentrations needed to halve the percentage of positive cells) the log
concentration / % positive cells curves were fitted using the equation modeling a symmetrical sigmoid;
this analysis enables to obtain the IC50 values with a 95% confidence interval. The significance of the
difference among IC50 values was determined by the F-test. Data were analyzed using GraphPad Prism, version 5.03 software (GraphPad Software Inc.).

Acknowledgements. This work was supported by grants from the Italian Ministry of Health and CARIPLO Foundation (533F/Q/1 and Guard, to M.S.) and from the Regione Piemonte (Progetti di Ricerca Sanitaria Finalizzata to P.C.). The kind gift of FMOC amino acids by Flamma S.p.A. (Bergamo, Italy) is gratefully acknowledged. The authors thank Laura Colombo and Alfredo Cagnotto
for peptide synthesis, Chiara Milan and Alessandra Roncaglioni for mass spectrometric and molecular
modeling studies.

Supporting Information

Additional Tables S1, S2 and Figures S1, S2, S3, S4, S5, S6, S7, S8 and S9 are described in the text. This material is available free of charge via the Internet at http://pubs.acs.org.

References

(1) Goldberg, A.L. Protein degradation and protection against misfolded or damaged proteins. *Nature* **2003**, *426*, 895-899.
(2) Goldberg, A.L.; Cascio, P.; Saric, T.; Rock, K.L. The importance of the proteasome and subsequent proteolytic steps in the generation of antigenic peptides. *Mol Immunol* **2002**, *39*, 147-164.
(3) Jung, T.; Catalgol, B.; Grune, T. The proteasomal system. *Mol Aspects Med* **2009**, *30*, 191-296.
(4) Konstantinova, I.M.; Tsimokha, A.S.; Mittenberg, A.G. Role of proteasomes in cellular regulation. *Int Rev Cell Mol Biol* **2008**, *267*, 59-124.
(5) Dahlmann, B. Role of proteasomes in disease. *BMC Biochem* **2007**, *8* Suppl 1, S3.
(6) Lehman, N.L. The ubiquitin proteasome system in neuropathology. *Acta Neuropathol* **2009**, *118*, 329-347.
(7) Burger, A.M.; Seth, A.K. The ubiquitin-mediated protein degradation pathway in cancer: therapeutic implications. *Eur J Cancer* **2004**, *40*, 2217-2229.
(8) Adams, J. The development of proteasome inhibitors as anticancer drugs. *Cancer Cell* **2004**, *5*, 417-421.
(9) D'Alessandro, A.; Pieroni, L.; Ronci, M.; D'Aguanno, S.; Federici, G.; Urbani, A. Proteasome inhibitors therapeutic strategies for cancer. *Recent Pat Anticancer Drug Discov* **2009**, *4*, 73-82.
(10) Voorhees, P.M.; Dees, E.C.; O'Neil, B.; Orlowski, R.Z. The proteasome as a target for cancer therapy. *Clin Cancer Res* **2003**, *9*, 6316-6325.
(11) Curran, M.P.; McKeage, K. Bortezomib: a review of its use in patients with multiple myeloma. *Drugs* **2009**, *69*, 859-888.
(12) Adams, J.; Palombella, V.J.; Sausville, E.A.; Johnson, J.; Destree, A.; Lazarus, D.D.; Maas, J.; Pien, C.S.; Prakash, S.; Elliott, P.J Proteasome inhibitors: a novel class of potent and effective antitumor agents. *Cancer Res* **1999**, *59*, 2615-2622.
(13) Kisselev, A.F.; Goldberg, A.L. Monitoring activity and inhibition of 26S proteasomes with fluorogenic peptide substrates. *Methods Enzymol* **2005**, *398*, 364-378.
(14) Dantuma, N.P.; Lindsten, K.; Glas, R.; Jellne, M.; Masucci, M.G. Short-lived green fluorescent proteins for quantifying ubiquitin/proteasome-dependent proteolysis in living cells. *Nat Biotechnol* **2000**, *18*, 538-543.
(15) Neefjes, J.; Dantuma, N.P. Fluorescent probes for proteolysis: tools for drug discovery. *Nat Rev*
Drug Discov **2004**, *3*, 58-69.
(16) Stack, J.H.; Whitney, M.; Rodems, S.M.; Pollok, B.A. A ubiquitin-based tagging system for controlled modulation of protein stability. *Nat Biotechnol* **2000**, *18*, 1298-1302.
(17) Arendt, C.S.; Hochstrasser, M. Identification of the yeast 20S proteasome catalytic centers and subunit interactions required for active-site formation. *Proc Natl Acad Sci U S A* **1997**, *94*, 7156-7161.
(18) Heinemeyer, W.; Fischer, M.; Krimmer, T.; Stachon, U.; Wolf, D.H. The active sites of the eukaryotic 20 S proteasome and their involvement in subunit precursor processing. *J Biol Chem* **1997**, *272*, 25200-25209.
(19) Dolenc, I.; Seemuller, E.; Baumeister, W. Decelerated degradation of short peptides by the 20S proteasome. *FEBS Lett* **1998**, *434*, 357-361.
(20) Derossi, D.; Calvet, S.; Trembleau, A.; Brunissen, A.; Chassaing, G.; and Prochiantz, A. Cell internalization of the third helix of the Antennapedia homeodomain is receptor-independent. *J Biol Chem* **1996**, *271*, 18188-18193.
(21) Jarver, P.; Langel, U. Cell-penetrating peptides--a brief introduction. *Biochim Biophys Acta* **2006**, *1758*, 260-263.
(22) Matayoshi, E.D.; Wang, G.T.; Krafft, G.A.; Erickson, J. Novel fluorogenic substrates for assaying retroviral proteases by resonance energy transfer. *Science* **1990**, *247*, 954-958.
(23) Corey, M.J.; Hallakova, E.; Pugh, K.; Stewart, J.M. Studies on chymotrypsin-like catalysis by

synthetic peptides. *Appl Biochem Biotechnol* **1994**, *47*, 199-210; discussion 210-212.
(24) Fenteany, G.; Standaert, R.F.; Lane, W.S.; Choi, S.; Corey, E.J.; Schreiber S.L. Inhibition of proteasome activities and subunit-specific amino-terminal threonine modification by lactacystin. *Science* **1995**, *268*, 726-731.
(25) Emmerich, N.P.; Nussbaum, A.K.; Stevanovic, S.; Priemer, M.; Toes, R.E.: Rammensee, H.G.; Schild, H. The human 26 S and 20 S proteasomes generate overlapping but different sets of peptide fragments from a model protein substrate. *J Biol Chem* **2000**, *275*, 21140-21148.
(26) Holzhutter, H.G.; Frommel, C.; Kloetzel, P.M. A theoretical approach towards the identification
of cleavage-determining amino acid motifs of the 20 S proteasome. *J Mol Biol* **1999**, *286*, 1251-1265.
(27) Frankel, A.D.; Pabo, C.O. Cellular uptake of the tat protein from human immunodeficiency virus. *Cell* **1988**, *55*, 1189-1193.
(28) Herce, H.D.; Garcia, A.E. Molecular dynamics simulations suggest a mechanism for translocation of the HIV-1 TAT peptide across lipid membranes. *Proc Natl Acad Sci U S A* **2007**, *104*, 20805-20810.
(29) Hanada, M.; Sugawara, K.; Kaneta, K.; Toda, S.; Nishiyama, Y.; Tomita, K.; Yamamoto, H.; Konishi, M.; Oki, T. Epoxomicin, a new antitumor agent of microbial origin. *J Antibiot (Tokyo)* **1992**, *45*, 1746-1752.
(30) Obeng, E.A.; Carlson, L.M.; Gutman, D.M.; Harrington, W.J. Jr; Lee, K.P.; Boise, L.H.. Proteasome inhibitors induce a terminal unfolded protein response in multiple myeloma cells. *Blood* **2006**, *107*, 4907-4916.
(31) Craiu, A.; Gaczynska, M.; Akopian, T.; Gramm, C.F.; Fenteany, G.; Goldberg, A.L.; Rock, K.L. Lactacystin and clasto-lactacystin beta-lactone modify multiple proteasome beta-subunits and inhibit intracellular protein degradation and major histocompatibility complex class I antigen presentation. *J Biol Chem* **1997**, *272*, 13437-13445.
(32) Kisselev, A.F.; Goldberg, A.L. Proteasome inhibitors: from research tools to drug candidates. *Chem Biol* **2001**, *8*, 739-758.
(33) Bianchi, G.; Oliva, L.; Cascio, P.; Pengo, N.; Fontana, F.; Cerruti, F.; Orsi, A.; Pasqualetto, E.; Mezghrani, A.; Calbi, V.; Palladini, G.; Giuliani, N.; Anderson, K.C.; Sitia, R.; Cenci, S. The proteasome load versus capacity balance determines apoptotic sensitivity of multiple myeloma cells to proteasome inhibition. *Blood* **2009**, *113*, 3040-3049.
(34) Cascio, P.; Oliva, L.; Cerruti, F.; Mariani, E.; Pasqualetto, E.; Cenci, S.; Sitia R. Dampening Ab
responses using proteasome inhibitors following in vivo B cell activation. *Eur J Immunol* **2008,** *38*, 658-667.
(35) Cenci, S.; Mezghrani, A.; Cascio, P.; Bianchi, G.; Cerruti, F.; Fra, A.; Lelouard, H.; Masciarelli,
S.; Mattioli, L.; Oliva, L.; Orsi, A.; Pasqualetto, E.; Pierre, P.; Ruffato, E.; Tagliavacca, L.; Sitia, R. Progressively impaired proteasomal capacity during terminal plasma cell differentiation. *EMBO J* **2006**, *25*, 1104-1113.
(36) Cenci, S.; Sitia, R. Managing and exploiting stress in the antibody factory. *FEBS Lett* **2007**, *581*, 3652-3657.
(37) Hanna, J.; Finley, D. A proteasome for all occasions. *FEBS Lett* **2007**, *581*, 2854-2861.
(38) Cascio, P.; Hilton, C.; Kisselev, A.F.; Rock, K.L.; Goldberg, A.L. 26S proteasomes and immunoproteasomes produce mainly N-extended versions of an antigenic peptide. *EMBO J* **2001**, *20*, 2357-2366.
(39) Pandey, U.B.; Nie, Z.; Batlevi, Y.; McCray, BA.; Ritson, G.P.; Nedelsky, N.B.; Schwartz, S.L.;
DiProspero, N.A.; Knight, M.A.; Schuldiner, O.; Padmanabhan, R.; Hild, M.; Berry, D.L.; Garza, D.; Hubbert, C.C.; Yao, T.P.; Baehrecke, E.H.; Taylor, J.P. HDAC6 rescues

neurodegeneration and provides an essential link between autophagy and the UPS. *Nature* **2007**, *447*, 859-863.
(40) Menendez-Benito, V.; Heessen, S.; Dantuma, N.P. Monitoring of ubiquitin-dependent proteolysis with green fluorescent protein substrates. *Methods Enzymol* **2005**, *399*, 490-511.
(41) Moravec, R.A.; O'Brien, M.A.; Daily, W.J.; Scurria, M.A.; Bernad, L.; Riss, T.L. Cell-based bioluminescent assays for all three proteasome activities in a homogeneous format. *Anal Biochem* **2009**, *387*, 294-302.
(42) Hara, T.; Nakamura, K.; Matsui, M.; Yamamoto, A.; Nakahara, Y.; Suzuki-Migishima, R.; Yokoyama, M.; Mishima, K.; Saito, I.; Okano, H.; and Mizushima, N. Suppression of basal autophagy in neural cells causes neurodegenerative disease in mice. *Nature* **2006**, *441*, 885-889.
(43) Komatsu, M.; Waguri, S.; Chiba, T.; Murata, S.; Iwata, J.; Tanida, I.; Ueno, T.; Koike, M.; Uchiyama, Y.; Kominami, E.; Tanaka, K. Loss of autophagy in the central nervous system causes neurodegeneration in mice. *Nature* **2006**, *441*, 880-884.
(44) Princiotta, M.F.; Finzi, D.; Qian, S.B.; Gibbs, J.; Schuchmann, S.; Buttgereit, F.; Bennink, J.R.; Yewdell, J.W. Quantitating protein synthesis, degradation, and endogenous antigen processing. *Immunity* **2003**, *18*, 343-354.
(45) Richard, J.P.; Melikov, K.; Vives, E.; Ramos, C.; Verbeure, B.; Gait, M.J.; Chernomordik, L.V.; Lebleu, B. Cell-penetrating peptides. A reevaluation of the mechanism of cellular uptake. *J Biol Chem* **2003**, *278*, 585-590.
(46) Cascio, P.; Goldberg, A.L. Preparation of hybrid (19S-20S-PA28) proteasome complexes and analysis of peptides generated during protein degradation. *Methods Enzymol* **2005**, *398*, 336-352.
(47) Kony, D.B.; Hunenberger, P.H.; van Gunsteren, W.F. Molecular dynamics simulations of the native and partially folded states of ubiquitin: influence of methanol cosolvent, pH, and temperature on the protein structure and dynamics. *Protein Sci* **2007**, *16*, 1101-1118.
(48) Rocchia, W.; Sridharan, S.; Nicholls, A.; Alexov, E.; Chiabrera, A.; Honig, B. Rapid grid-based
construction of the molecular surface and the use of induced surface charge to calculate reaction field energies: applications to the molecular systems and geometric objects. *J Comput Chem* **2002**, *23*, 128-137.
(49) Repici, M.; Mare, L.; Colombo, A.; Ploia, C.; Sclip, A.; Bonny, C.; Nicod, P.; Salmona, M.; Borsello, T. c-Jun N-terminal kinase binding domain-dependent phosphorylation of mitogenactivated
protein kinase kinase 4 and mitogen-activated protein kinase kinase 7 and balancing cross-talk between c-Jun N-terminal kinase and extracellular signal-regulated kinase pathways in cortical neurons. *Neuroscience* **2009**, *159*, 94-103.

Table 1. Percentage of Fluorescent Positive Cells after TED Treatment, with or without Epoxomicin.

	% of positive cells − epoxomicin mean ± SEM	% of positive cells + epoxomicin mean ± SEM
HeLa	77.3 ± 1.4	17.0 ± 1.5***[d]
N2a	47.1 ± 1.5	16.5 ± 4.2**[c]
MM.1S	37.6 ± 1.4	18.3 ± 3.2**[c]
U266	43.0 ± 1.7	23.7 ± 3.4**[c]
hippocampal neurons	86.7 ± 4.9	52.2 ± 2.2*[b]

Cells were incubated for 15 min with 17 μM TED, in the presence or absence of 5 μM of the proteasome inhibitor epoxomicin. The number of positive cells is expressed as percentage of total cells.
Data are mean ± standard error of the mean (SEM) of three independent experiments, each performed
with at least 100 cells; * $P < 0.05$; ** $P < 0.01$; *** $P < 0.001$, unpaired *t*-test.

Figure Legends
Figure 1. Schematic Structure of TED. Primary amino acid sequence, showing linkage of fluorophores
DABCYL and EDANS to Lys 2 and Glu 10, respectively. The blue arrow indicates the preferred cleavage site, yellow arrows the secondary primed regions and red dashed arrows the non-primed regions. Residues 48-57 of the TAT protein were linked to the side chain of Glu 10 at the C-terminus.
D-amino acids are in position 1,3,4.
Figure 2. Mass Spectrometric Analysis of TED Degradation Products. HeLa cells were incubated with
17 μM TED for 15 min at 37 °C and cell lysates were analyzed by MALDI-TOF MS. (A) The molecular ion at m/z 3084.48 corresponds to uncleaved TED $[M+H]^+$. (B) The molecular ion at m/z 1270.97 corresponds to cleavage of TED at the carboxyl end of the Tyr at position 8. The molecular ion
at m/z 1141.58 corresponds to TED cleavage both at the Tyr residue and the N-terminal Lys residue and the molecular ion at m/z 2046.43 corresponds to the peptide from cleavage between the two Lys at
positions 13 and 14 in the TAT sequence. Uncleaved TED molecular ion $[M+H]^+$ was negligible at m/z
3084.97.
Figure 3. TED Internalization and Cleavage in U266 Cells. (A) Representative micrographs showing
progressive TED internalization and cleavage after 0, 5 and 15 min incubation with 17 μM TED. Peptide cleavage resulted in significant EDANS fluorescence increase, monitored by time-lapse recording microscopy. Pre-incubation for 3 h with 5 μM of the proteasome inhibitor epoxomicin, followed by co-incubation with TED for 15 min, significantly prevented EDANS fluorescence. Scale

bar: 50 μm. (B) Quantification of fluorescence-positive U266 cells after 15 min incubation with TED.
Treatment with epoxomicin significantly reduced the number of positive cells; ** $P < 0.01$, unpaired *t*-test. Data are mean ± standard error of the mean (SEM) from three independent experiments. (C) Flowcytometry
of EDANS and GFP fluorescence in Ub^{G76V}GFP-U266 cells incubated with 17 μM TED for 15 min, in the presence or absence of 5 μM epoxomicin. Incubation with TED alone resulted in increased EDANS mean fluorescence intensity (MFI), which was partially prevented by pre-treatment
with epoxomicin; no fluorescence was detected in untreated cells (CTR). GFP fluorescence was barely
detectable in untreated cells (CTR), but accumulated upon pre-treatment with epoxomicin.

Figure 4. Dose-Response Curves of TED Cleavage Inhibition. HeLa cells were pre-incubated for 3 h
with different concentrations of epoxomicin (Epox from 0.5 to 20 μM), MG-132 (from 1 to 20 μM) or
bortezomib (BTZ from 0.01 to 1 μM), and then treated with 17 μM TED for 15 min. Quantification of
fluorescence-positive cells was carried out at each inhibitor concentration on 50-70 cells from 8-10 images. The IC50 of the inhibitors were 13.08 μM for epoxomicin, 6.45 μM for MG-132 and 141.3 nM
for bortezomib (p=0.0016, F=14.26). Results are expressed as mean ± standard error of the mean (SEM) from two independent experiments.

Figure 5. Intracellular Distribution of TED in Primary Hippocampal Neurons and U266 Multiple Myeloma Cells. (A) Cells were pre-incubated for 5 min at 37 °C with 1 μM SYTO59 to stain cell nuclei, followed by 15 min incubation with 17 μM TED. EDANS fluorescence was monitored by timelapse
recording microscopy. EDANS, green; SYTO59, red; co-localization of TED and SYTO59 is shown by merged micrographs (third column). Scale bar: 20 μm. (B) Pseudocolor images with localization of TED in the nucleus of hippocampal neurons, as indicated by a color shift from blue to
red, with a more homogeneous distribution in U266 cells. Micrographs showing intracellular localization of TED and pseudocolor images for different cell lines are in Figure S8.

Figure 6. Time-course of TED Cleavage Efficiency in MM.1S and U266 Multiple Myeloma Cell Lines. Cells were incubated with 17 μM TED for 30 min and EDANS fluorescence changes monitored
by flow cytometry for 30 min. Data were acquired every 3 min. Mean fluorescence intensity (MFI) progressively increased over incubation, with lower values in MM.1S than U266 cells at every time point. Two representative time points are shown. The number of positive cells/channel was also lower
in MM.1S than U266 cells. Data are from one representative experiment of two.

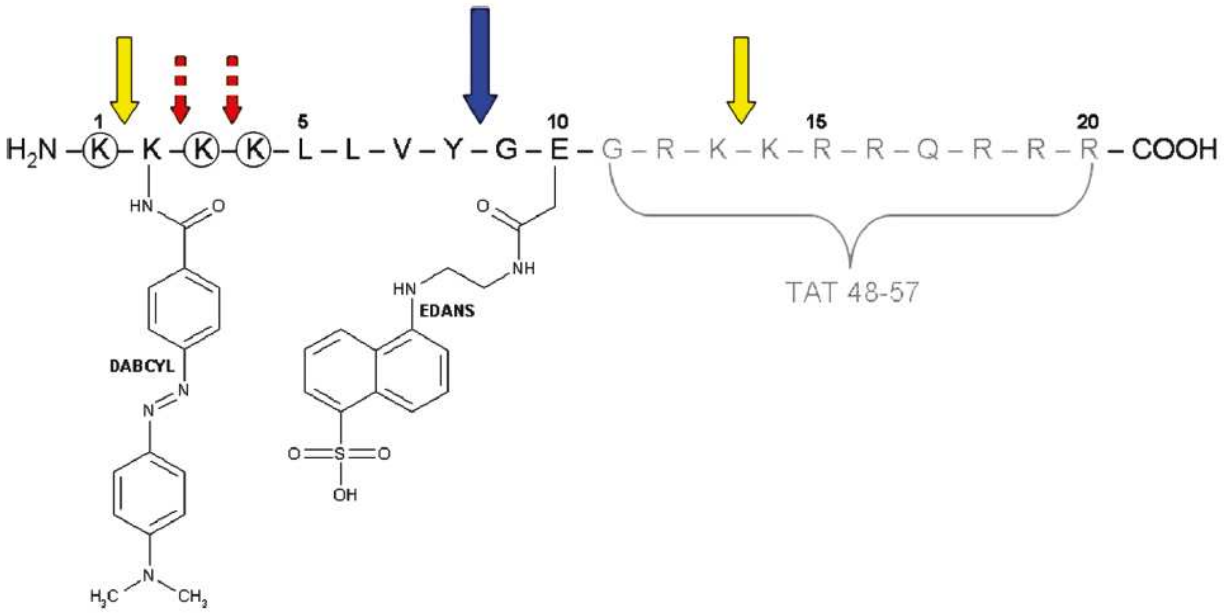

Figure 1

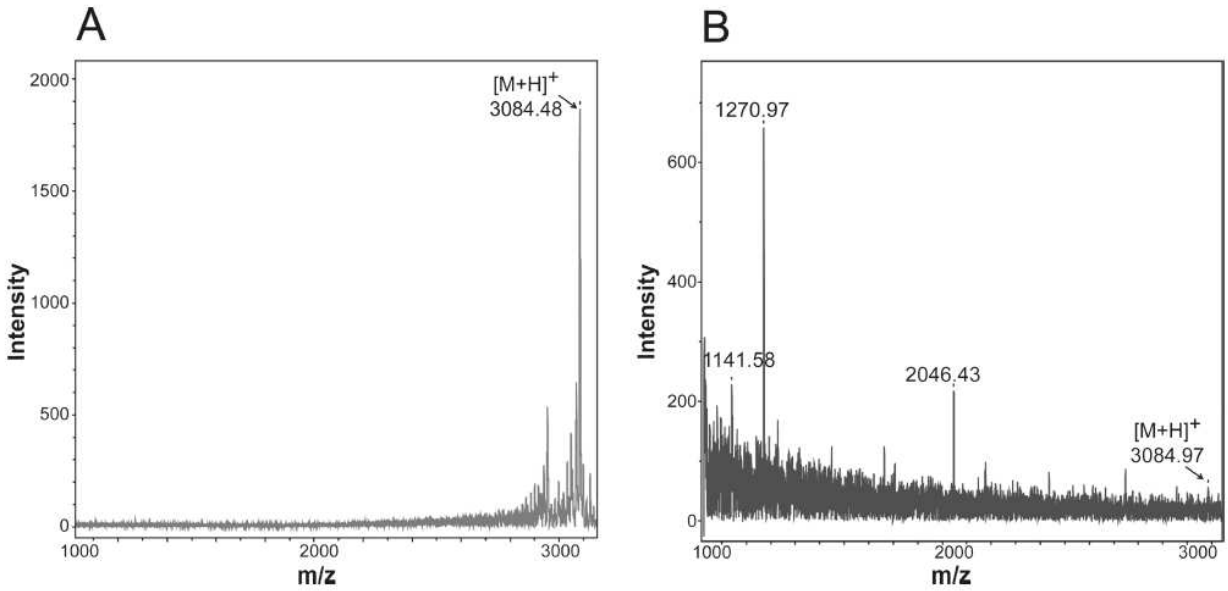

Figure 2

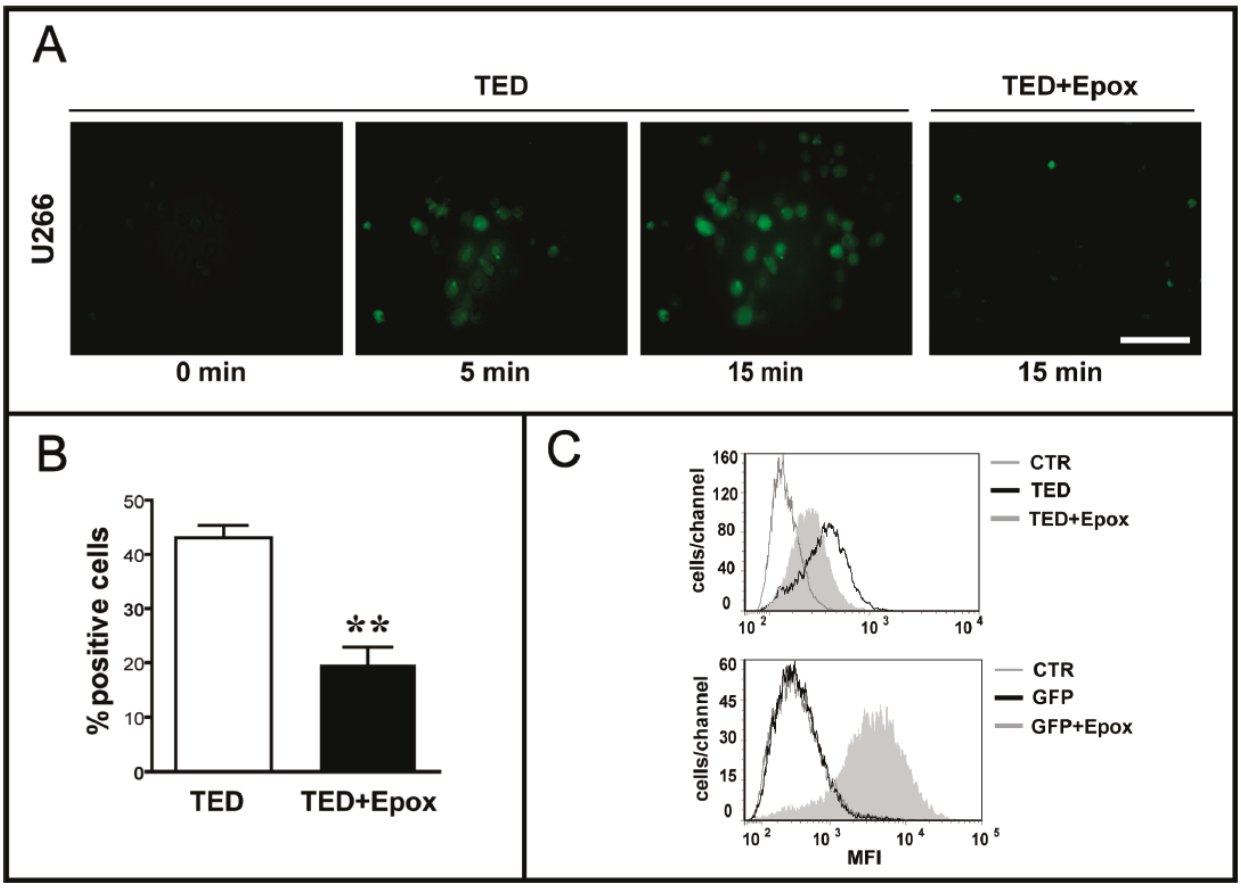

Figure 3

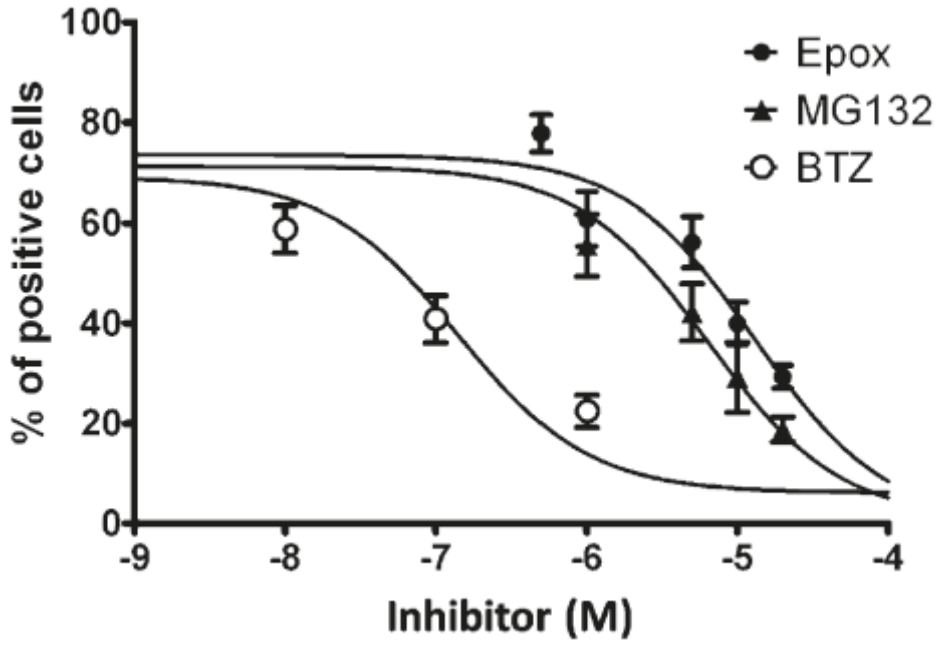

Figure 4

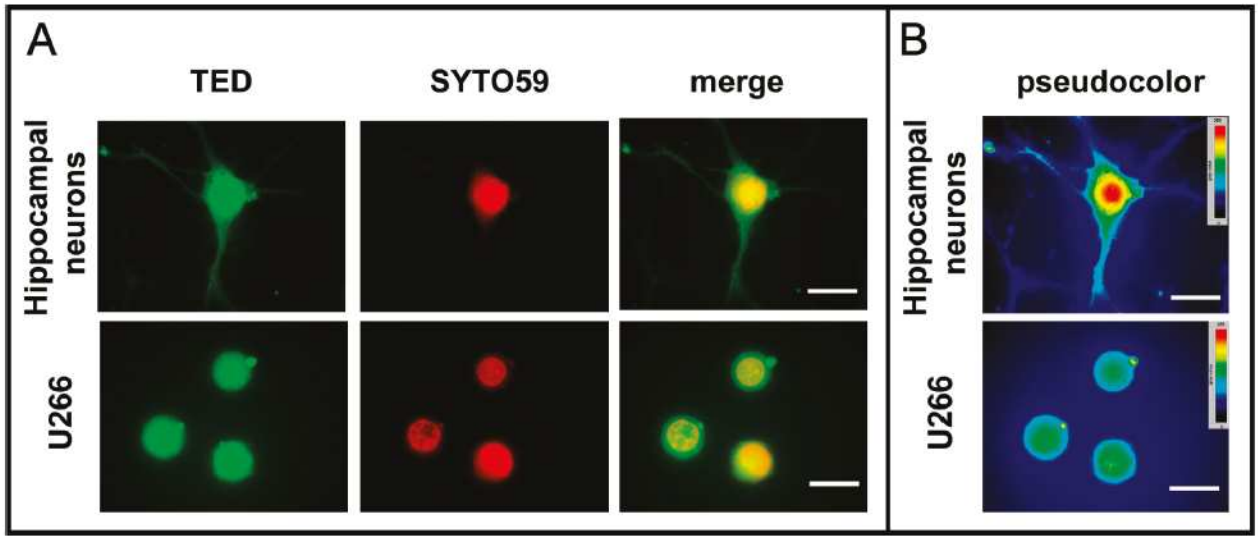

Figure 5

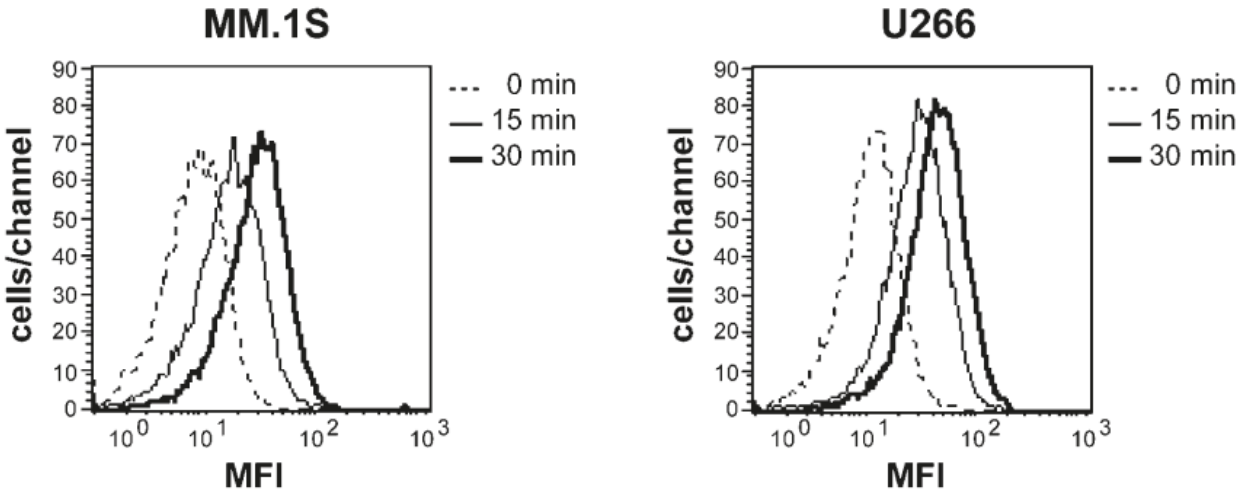

Figure 6